tion zones; in our case we can speculate that, since also the smectic form in the liquid is permeable to the penetrant, the two different zones of the various curves refer to the interaction with either the amorphous or the smectic form of iPP.

In order to draw more thorough conclusions further investigations are needed on the crystallization kinetics in these solvents and on the growing crystalline structure.

Acknowledgment. We thank Prof. R. Zannetti for many helpful discussions.

Registry No. iPP, 25085-53-4.

References and Notes

(1) Kashmiri, M. I.; Sheldon, R. P. *Br. Polym. J.* **1969**, *1*, 65.
(2) Zachmann, H. G. *Faserforsch. Textiltech.* **1967**, *18*, 95.
(3) Zachmann, H. G. *Kolloid Z. Z. Polym.* **1963**, *189*, 67.
(4) Desai, D. B.; Wilkes, G. L. *J. Polym. Sci., Polym. Symp.* **1974**, *46*, 291.
(5) Wilkes, G. L.; Parlapiano, J. *Polym. Prepr. (Am. Chem. Soc., Div. Polym. Chem.)* **1976**, *17*(2), 937.
(6) Alfrey, T., Jr.; Gurnee, E. F.; Lloyd, W. G. *J. Polym. Sci.* **1966**, *C12*, 249.
(7) Overbergh, N.; Berghmans, H.; Smets, G. *Polymer* **1975**, *16*, 703.
(8) Makarewicz, P. J.; Wilkes, G. L. *J. Polym. Sci., Polym. Phys. Ed.* **1978**, *16*, 1529.
(9) Titow, W. V.; Braden, M.; Currell, B. R.; Loneragan, R. J. *J. Appl. Polym. Sci.* **1974**, *18*, 867.
(10) Turska, E.; Benecki, W. *J. Polym. Sci., Polym. Symp.* **1974**, *44*, 59.
(11) Ware, R. A.; Tirtowidjojo, S.; Cohen, C. *J. Appl. Polym. Sci.* **1981**, *26*, 2975.
(12) Turska, E.; Janeczek, J. *Polymer* **1979**, *20*, 355.
(13) Natta, G.; Peraldo, M.; Corradini, P. *Atti Accad. Naz. Lincei, Cl. Sci. Fis., Mat. Nat., Rend.* **1956**, *26*, 14.
(14) Miller, R. L. *Polymer* **1959**, *1*, 135.
(15) Bodor, G.; Grell, M.; Kello, A. *Faserforsch. Textiltech.* **1964**, *15*, 527.
(16) Wunderlich, B.; Grebowicz, J. *Adv. Polym. Sci.* **1984**, *60/61*, 1.
(17) Grebowicz, J.; Lau, J. F.; Wunderlich, B. *J. Polym. Sci., Polym. Symp.* **1984**, *71*, 19.
(18) Zannetti, R.; Celotti, G.; Fichera, A.; Francesconi, R. *Makromol. Chem.* **1969**, *128*, 137.
(19) Hendra, P. J.; Vile, J.; Willis, H. A.; Zichy, V.; Cudby, M. E. A. *Polymer* **1984**, *25*, 785.
(20) Vittoria, V. *Polym. Commun.* **1985**, *26*, 213.
(21) Rebenfeld, L.; Makarewicz, P. J.; Weighmann, H. D.; Wilkes, G. L. *J. Macromol. Sci., Rev. Macromol. Chem.* **1976**, *C15*(2), 279.
(22) Gardon, J. L. *Encycl. Polym. Sci. Technol.* **1967**, *12*, 627.
(23) Gezovich, D. M.; Geil, P. H. *Polym. Eng. Sci.* **1968**, *8*, 202.
(24) Kapur, S.; Rogers, C. E. *J. Polym. Sci., Polym. Phys. Ed.* **1972**, *10*, 2107.
(25) Baum, J. S.; Schultz, J. M. *J. Appl. Polym. Sci.* **1981**, *26*, 1579.
(26) Vittoria, V. *J. Polym. Sci.*, in press.
(27) Kambour, R. P.; Karasz, F. E.; Daane, J. H. *J. Polym. Sci., Polym. Phys. Ed.* **1966**, *4*, 327.
(28) Turska, E.; Benecki, W. *J. Appl. Polym. Sci.* **1979**, *23*, 3489.
(29) Durning, C. J.; Russel, W. B. *Polymer* **1985**, *26*, 119.
(30) Crank, J. *The Mathematics of Diffusion*; Oxford University Press: London, 1975.
(31) Jameel, H.; Waldman, J.; Rehenfeld, L. J. *J. Appl. Polym. Sci.* **1981**, *26*, 1795.
(32) Jameel, H.; Noether, H.; Rebenfeld, L. J. *J. Appl. Polym. Sci.* **1982**, *27*, 773.
(33) Vieth, W.; Wuerth, W. F. *J. Appl. Polym. Sci.* **1960**, *13*, 685.
(34) Hayes, R. A. *J. Appl. Polym. Sci.* **1961**, *5*, 318.
(35) Vocks, J. F. *J. Polym. Sci., Part A* **1964**, *2*, 5319.
(36) Alexander, L. E. *X-Ray Diffraction Methods in Polymer Science*; Wiley-Interscience: New York, 1969.
(37) Moore, W. R.; Sheldon, R. P. *Polymer* **1961**, *2*, 315.

Molecular Weight Distribution Dependence of the Viscoelastic Properties of Linear Polymers: The Coupling of Reptation and Tube-Renewal Effects

J. P. Montfort,* G. Marin, and Ph. Monge

Institut Universitaire de Recherche Scientifique, Laboratoire de Physique des Matériaux Industriels, Université de Pau et des Pays de l'Adour, 64000 Pau, France.
Received November 1, 1985

ABSTRACT: Considering that the terminal relaxation of every chain in a linear melt is dominated by reptational and constraint release motions, we propose an expression for the relaxation modulus $G(t)$ of entangled polymers as a function of the molecular weight distribution (MWD). The expressions of zero-shear viscosity η_0 and steady-state compliance J_e^0 derived from $G(t)$ describe correctly the experimental behavior: η_0 scales with average molecular weight as $\eta_0 \propto M_w^{3.4-3.8}$ for a constant polydispersity P; J_e^0 increases strongly with P and varies widely with the shape of MWD. We also predict a decrease of viscosity with polydispersity; this is a possible explanation of some experimental variations of viscosity, which do not follow the classical power law with M_w. The behavior expected for strictly monodisperse samples shows that it is necessary to consider a relaxation times distribution in the terminal region.

Introduction

It is well-known that the viscoelastic properties of polymers depend mainly on their molecular weight distributions (MWD). Experimental data on the molecular weight dependence of zero-shear viscosity η_0 generally support the power law $\eta_0 \propto M_w^{3.4}$ for binary blends of narrow distribution samples,[1-3] but results differ for broad distribution samples. Data for high-density polyethylene[4] agree with the above expression, whereas commercial polystyrenes[5,6] follow higher power laws: $M_w^{5.25}$ or $M_w^{5.7}$.

The steady-state compliance J_e^0 is very sensitive to molecular weight distribution, especially to the tail of the distribution at high molecular weights. The increase of J_e^0 with the broadness of the distribution can reach 2 or 3 orders of magnitude for binary blends whose components are very different in molecular weight.[1,7,8]

Several blending laws have been proposed to account for the behavior of binary blends.[9-11] Masuda et al.[12] reviewed them, discussed their applicability, and suggested some improvements. These theories are based on a linear

0024-9297/86/2219-1979$01.50/0

or quadratic combination of the relaxation spectrum $H_i(\tau_i)$ of each component and, for quadratic laws, of an interaction spectrum H_{ij}. The interactions between chains with different molecular weights by means of entanglements justify the shift factors λ_i by which the relaxation time of each component is modified and also the introduction of an interaction spectrum in the quadratic expression. The same argument was applied to the transient-network model proposed earlier by Hong et al.[13,14] for monodisperse polymers. It involves a modification of the relaxation times for each component, depending on the composition of the blend.[15] But the expression of the modified relaxation times is not explicitly related to the pure individual relaxation times and to the weight fractions. This model has been successful for binary blends of narrow distribution polymers and has been extended to polydisperse homopolymers.[16]

Kurata[17] proposed recently a blending law very close to the quadratic expressions, starting from the tube model of Doi and Edwards,[18] but only the higher molecular weight term is shifted toward low relaxation times. He considers the reptation of the longer chains within a fixed tube imposed by the other long chains, in a time scale where the short chains–long chains entanglements become ineffective. Other diffusion mechanisms, mainly tube renewal, are considered by Watanabe et al.,[19,20] but some determinations of relaxation times and terms of the relaxation spectra are questionable. The contribution of the surrounding chains of the diffusion of each chain imbedded in the tube is analyzed by Marrucci[21] in a different way. He postulates that after an instantaneous strain the tube diameter must be taken as an increasing function of time during relaxation. The relaxation function $F(t)$ of the Doi–Edwards theory is therefore modified, and a nonexponential relaxation modulus $G(t)$ is obtained. This picture applied to the polydisperse case allows one to forecast the variations of the viscosity with the composition of the blend. For a binary blend, the previsions are not far from the experimental observations, i.e., $\eta_0 \propto M_w^{3.4}$.

We have proposed recently,[8] in the tube-model area, an expression for the tube-renewal time of an N-chain in an N–N_S binary blend based on Graessley's model.[22] We have derived the variations of zero-shear viscosity η_0 and steady-state compliance J_e^0 for binary blends of narrow distribution samples. In the present paper, our model is improved in this way:[23] an expression for the relaxation modulus $G(t)$ is established in a simplified form, considering the behavior of the entanglement network of a binary blend. This model is extended to the polydisperse case. For broad distribution polymers, the variations of η_0 and J_e^0 with the width of the MWD are calculated and compared with experimental data.

The model we propose does not take into account a distribution of relaxation times; this would not, however, change fundamentally the conclusions, as Marrucci[21] pointed out. But for describing the whole terminal and plateau regions, it would be necessary to consider such a distribution and, moreover, mechanisms other than reptation and tube renewal. For example, tube-length fluctuations may explain the experimental law $\eta_0 \propto M^{3.4}$.[34,35] They depend only on the length of the N-chain and no on its environment, as for the pure reptational diffusion. So, in this paper, the tube-disengagement time is considered as including reptation and tube-length fluctuation ($\tau_d \propto M^{3.3}$).[8]

I. Binary Blends of Narrow Distribution Samples

1. Relaxation Modulus $G(t)$. In the Doi–Edwards theory[18] established for monodisperse samples, $G(t)$ is defined as the product of the plateau modulus G_N^0 and the relaxation function given by

$$F(t) = \frac{8}{\pi^2} \sum_{n\,\mathrm{odd}} \frac{1}{n^2} \exp(-n^2 t/\tau_d) \qquad (1)$$

where τ_d is the tube-disengagement time or reptation time. If L is the curvilinear length of the tube and a its diameter, τ_d is found proportional to $(L/a)^3$. The rheological implications of the model show that the term for $n = 1$ dominates. The plateau modulus is a measure of the temporary network density of entanglements. It is defined by

$$G_N^0 = \frac{3}{5}\rho \frac{RT}{M}\left(\frac{L}{a}\right) \qquad (2)$$

where ρ is the polymer density and L/a represents the number of submolecules separated by entanglements. If M_e is the molecular weight of every submolecule, then $N = M/M_e$. For concentrated polymer solutions, the entanglement density decreases with concentration according to $M_e' = M_e/\phi$, ϕ being the weight fraction of the polymer. Thus, the plateau modulus varies with concentration and molecular weight as

$$G_N^0 \propto \phi^2 M^0 \qquad (3)$$

The experimental determination of G_N^0 in polymer melts can be made by integration of either the relaxation spectrum $H(\tau)$[24] or the loss modulus $G''(\omega)$[25] in the terminal region only. Large molecular weights are required to separate the transition and terminal relaxations.

In another way, if the onset of the transition region is well-defined, the inflection point of the curve of $G'(\omega)$ defines also the plateau modulus G_N^0: if we plot the variations of the slope of the master curves of $G'(\omega)$ for all narrow distribution polystyrene samples studied,[8,23] as shown in Figure 1 for sample F20, we confirm the value of $G_N^0 = (2.0 \pm 0.1) \times 10^6$ dyn cm^{-2} for polystyrene and its molecular weight independence.

The concentration dependence obeys the power law $G_N^0 \propto \phi^2$ for some polymers, for example, poly(methyl methacrylate)[26] and polyisoprene,[27] but in other cases, for example, polyethylene (PE), polybutadiene (PB), and hydrogenated polybutadiene (HPB),[25] the results support a

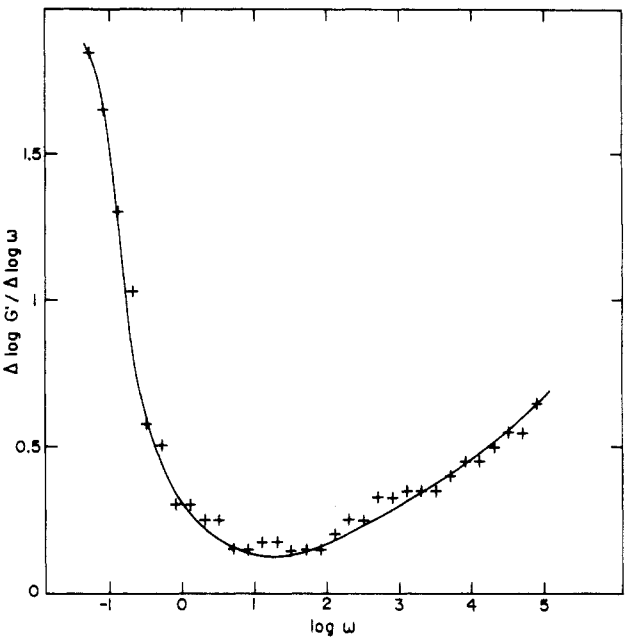

Figure 1. Determination of plateau modulus G_N^0 from the inflection point of $G'(\omega)$ for the sample F20[8] at T = 160 °C.

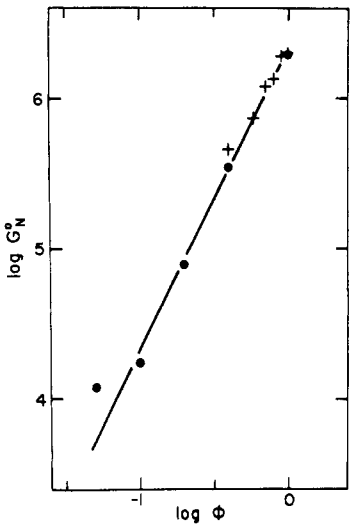

Figure 2. Plateau modulus G_N^0 for concentrated PS–PS solutions: (●) F90 in F008; (+) F11 in F002 and in F018.

Table I
Elastic Properties of Binary Blends of Polystyrene

sample	ϕ	$J_e'^0$, cm^2 dyn^{-1}	G_N^0, dyn cm^{-2}	$J_e'^0 G_N^0$
F90 (M = 900 000) in F008 (M = 8500)	0.05	4.0×10^{-4}	1.25×10^4	5.0
	0.10	1.4×10^{-1}	1.8×10^4	2.5
	0.20	5.0×10^{-5}	8×10^4	4.0
	0.40	8.0×10^{-6}	3.4×10^5	2.6
	1	2.1×10^{-6}	2.0×10^6	4.2
F11 (M = 110 000) in F002 (M = 2000)	0.40	6.6×10^{-6}	4.7×10^5	3.1
	0.60	2.9×10^{-6}	6.8×10^5	2.0
	0.80	1.8×10^{-6}	1.35×10^6	2.4
	0.90	1.4×10^{-6}	1.8×10^6	2.5
	1	1.25×10^{-6}	2.0×10^6	2.5
F11 (M = 110 000) in F018 (M = 17 500)	0.70	2.2×10^{-6}	1.25×10^6	2.8

slightly strong dependence, $G_N^0 \propto \phi^{2.22-2.26}$. In a previous study of binary blends of high molecular weight polystyrene in low molecular weight polystyrene,[28] we have shown that $J_e^0 \propto \phi^{-2}$, in agreement with the Doi–Edwards previsions. For the same blends, we have represented in Figure 2 the concentration dependence of G_N^0. The data, listed in Table I, agree with the quadratic law (relation 3), confirming assumptions that G_N^0 is proportional to the concentration of binary contacts between segments of the high molecular weight chains. The entanglement network of these chains is responsible for the rubberlike elastic response in the intermediate region between the terminal and transition zones. In contrast, the variations of the storage modulus for binary blends of high molecular weight polystyrene ($M_1 > M_2 > M_c \simeq 2M_e$) show two plateau moduli in the terminal region as shown in Figure 3. At the highest frequencies curves tend to merge, reaching the plateau modulus G_N^0 of monodisperse samples at the frequency ω_{pl} separating the terminal and transition regions. All the chains participate in the entanglement network, giving a rubberlike response in that scale of frequencies. At an intermediate frequency, ω_{pl}', a clear inflection in the curve defines a plateau modulus $G_N'^0$ associated with the low-frequency relaxation domain. Data listed in Table II and shown in Figure 4 support a power law $G_N'^0 = G_N^0 \phi_1^{2.23}$, omitting the lowest point corresponding to $\phi_1 = 0.02$. The exponent is very close to those obtained for PE, PB, and HPB concentrated solutions.[25] It suggests strongly that the intermediate plateau modulus $G_N'^0$ is due essentially to binary contacts between the largest 1-chains. Then, at frequencies of the order of ω_{pl}',

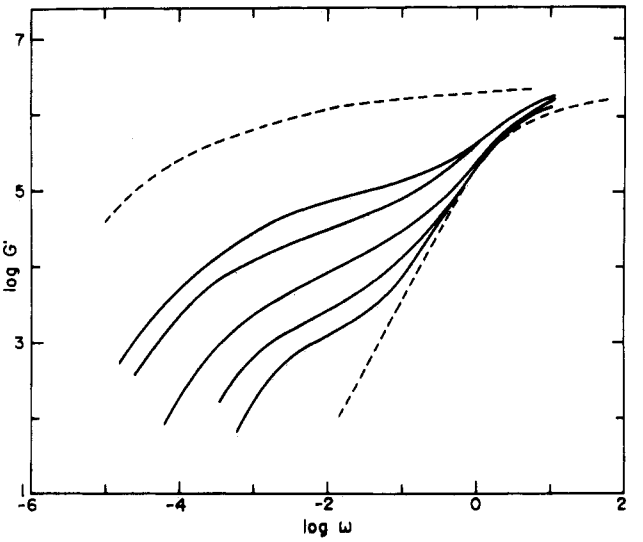

Figure 3. Master curves of $G'(\omega)$ at T = 160 °C for blends F10–F270. Dashed lines are for pure fractions; full lines are for blends.

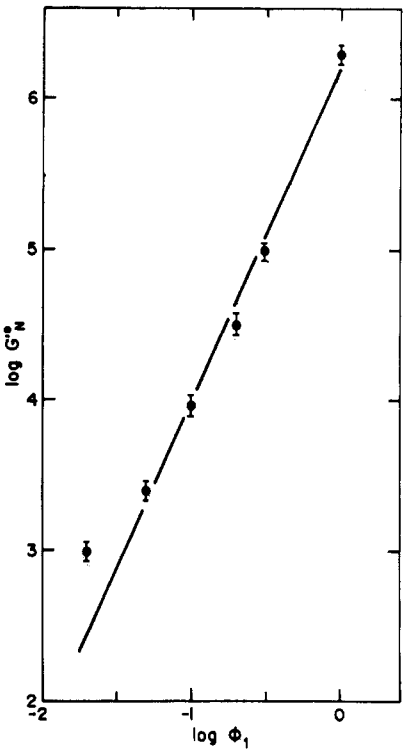

Figure 4. Concentration dependence of intermediate plateau modulus $G_N'^0$ for blends F10–F270; ϕ_1 is the F270 concentration.

Table II
Plateau Modulus of Binary Blends of Polystyrene[a]

ϕ_1	$G_N'^0$, dyn cm^{-2}	ω_{pl}'
0.02	1×10^3	8×10^{-3}
0.05	2.5×10^3	9×10^{-3}
0.10	9.3×10^3	1.2×10^{-2}
0.20	3.2×10^4	1×10^{-2}
0.31	1×10^5	2.5×10^{-2}
1	2×10^6	5×10^{-1}

[a] M_1 = 2 700 000; M_2 = 100 000.

a rubberlike response appears in the terminal region because the 1–1 entanglements act as cross-links in that scale of frequencies. At $\phi_1 = 0.02$, the average molecular weight between two 1–1 entanglements, namely $M_e' = M_e \phi_1^{-1}$, is 900 000 for polystyrene and, in the blend studied (Table II), $M_1 = 3M_e'$. This value corresponds to the onset of

entanglement effects and, in this case, the 1–1 entanglement network is not fully constituted. Plateau modulus $G_N'^0$ of $\phi_1 = 0.02$ included, therefore, effects of the lowest molecular weight 2-chains.

At all concentrations in binary blends of narrow distribution samples of high molecular weight ($M_1 > M_2 > M_c$), the intermediate plateau separates two terminal relaxations. For $\omega < \omega_{pl}'$, only the high molecular weight 1-component exhibits viscoelastic properties, and the low molecular weight 2-component acts as a pure viscous liquid. For $\omega_{pl}' < \omega < \omega_{pl}$, the entanglement network of the 1-chains brings an elastic response, while 2-chains act as a viscoelastic liquid. For $\omega \sim \omega_{pl}$, all the chains participate in the entanglement network, and the plateau modulus G_N^0 is reached.

In other words, after a sudden strain, the 2-chains relax first in a time scale $[(\omega_{pl})^{-1}; (\omega_{pl}')^{-1}]$, and the 1-chains are fixed like strands of a rubber network. Then, for $t > (\omega_{pl}')^{-1}$, the 1-chains relax, while the 2-chains have restored their equilibrium configuration.

Assuming the additivity of the two components contributions to the relaxation modulus $G(t)$, we can write

$$G(t) = G_N'^0 F_1(t) + (G_N^0 - G_N'^0) F_2(t) \quad (4)$$

For simplicity, we will consider that $G_N'^0$ scales as ϕ_1^2 and will not take into account the relaxation time distribution in F_1 and F_2 (relation 1).

Then, $G(t)$ may be rewritten as

$$G(t) = G_N^0[\phi_1^2 \exp(-t/\tau_1) + (1 - \phi_1^2) \exp(-t/\tau_2)] \quad (5)$$

with the relaxation times τ_1 and τ_2 satisfying the condition

$$\tau_1 > (\omega_{pl}')^{-1} > \tau_2 > (\omega_{pl})^{-1} \quad (6)$$

Equation 5 above is absolutely similar to the expression of $H(\tau)$ proposed by Kurata.[17] Other blending laws[19,37] suggest a contribution of the short chain proportional to the weight (or volume) fraction and even cross terms. But, there is a lack of experimental evidences of that assumption. Only Prest[11] showed that a linear blending law fitted the experimental data with a weighting factor of the low-component term proportional to the volume fraction of the low component. There is, however, some uncertainty in the determination of the four empirical parameters involved in the pression of $H(\tau)$ obtained by means of approximation calculations. Equation 5 above does not include cross terms, but the coupling between chains of different lengths is assumed to be contained in the effect of the environment of every chain on its relaxation time. That is the effect of the tube-renewal mechanism.

2. Relaxation Times. In the pure reptation model, the relaxation time of a given N-chain is independent of the length of the surrounding chains. Recent theories[22,29,30] have considered the effect of tube renewal due to the reptation of the surrounding chains. The corresponding relaxation time τ_t varies as

$$\tau_t = N^2 \tau_w \propto N^2 N_S^3 \quad (7)$$

where τ_w is an average time for constraint release, proportional to the reptation time τ_d of the N_S-chains constituting the matrix.

For an N-chain embedded in an N_S-matrix, we have found experimentally for polystyrene[8]

$$\tau_t \propto M^{1.9} M_S^{2.3} \quad (8)$$

in the following molecular weight range: $35\,000 < M_S < 390\,000$ and $390\,000 < M < 3\,800\,000$. This relaxation time was calculated from an average relaxation time of the relaxation domain due to the presence of the long N-chains, as clearly shown in the plot of complex viscosities. In a different way, Watanabe et al.[38] calculate the contributions ΔA_G and $\Delta\eta_0$ of the N-chains to the elastic coefficient and zero-shear viscosity of dilute polystyrene blends. The ratio $\Delta A_G/\Delta\eta_0$ is also an average relaxation time of the N-chains. A careful examination of their data in the range $23\,400 < M_S < 72\,400$ and $427\,000 < M < 2\,810\,000$ gives the result

$$\tau_t \propto M^{1.8} M_S^{2.6} \quad (8a)$$

with values about 3 times ours at the same temperature. So, there is a discrepancy between experimental and theoretical exponents for N_S. We explained that[8] by the occurrence of correlated constaints due to multiple contacts between two chains N and N_S.

Using a similar topological argument, Klein[31] shows that within each blob of an N-chain containing n_S monomers (n_S is the number of monomers in an N_S-chain), the number p_i of different N_S-chains contributing to constraints on the N-chain within each blob is roughly $n_S^{1/2}$. So, only $n_S^{1/2}$ contacts are independent, and Klein postulates that the relaxation time of every neighboring constraint will be decreased by the same factor $n_S^{1/2}$. This argument applied to each effective entanglement constraint gives a tube-renewal time varying as

$$\tau_t \propto N^2 N_S^{2.5} \quad (9)$$

assuming $\tau_w \propto \tau_d(N_S) \propto N_S^3$. But, experimentally, τ_d scales as $N_S^{3.4}$, and then the decrease of the tube-renewal time is by a factor N_S rather than by a factor $N_S^{1/2}$. On the other hand, Klein pointed out that the effective entanglement constraints are taken every n_e monomers. So, if these constraints consisted of individual N_S-chains, there would be (n_S/n_e) of them by blob, and they could be assumed to be independent as long as $n_S/n_e < n_S^{1/2}$. This occurs, for polystyrene, for molecular weights M_S lower than about 3×10^6 ($M_e = 18\,000$), which is the usual case. Yet, experimental results mentioned above show that the assumption of correlated constraints holds even for low molecular weights. That could be proof that localized entanglement constraints do not really exist. They should be considered as a simplified picture of the more complex intermolecular interactions.

With a renormalization of the distance between effective constraints, we can derive that the tube-renewal time is decreased by a factor N_S. According to Klein,[31] a blob of n_S monomer of an N-chain is constrained by $n_S^{1/2}$ different N_S-chains. We assume that the number of effective constraints within a blob is equal (or at least proportional) to the number of the individual N_S-chains or, in other words, that all the N–N_S contacts relative to the same N_S-chain are removed together or in a shorter time than its reptation time. The distance, then, between two effective constraints is $n_S^{1/2}$ and not n_e. There will be $N' = n/n_S^{1/2}$ submolecules in the equivalent Rouse N-chain, and correlatively, the tube-renewal time will be

$$\tau_t = N'^2 \tau_w \propto N'^2 \tau_d(N_S)$$

Experimentally, $\tau_d(N_S)$ is proportional to $M_S^{3.4}$, and our analysis gives

$$\tau_t \propto M^2 M_S^{2.4} \quad (9a)$$

for $M_S < M$ and $n_e > n_S^{1/2}$, in very good agreement with the experimental data (relations 8 and 8a). For a highly entangled matrix ($n_S^{1/2} > n_e$), there are two modifications. According to Klein, all the constraints are due to different N_S-chains, so they are uncorrelated and we assume, following Doi, that tube-length fluctuations are negligible.

$\tau_d(N_S)$ is proportional to N_S^3, and the number of effective constraints is proportional to n only. A numerical simulation made by Marin[39] shows that the number of physical cross-links between an N-chain and an N_S-chain is proportional to $N_S^{1/2}$, but a decrease of the tube-renewal time is by a factor N_S if one postulates that all constraints relative to the same N_S-chain are removed together.

Considering the two processes, tube disengagement and tube renewal, Graessley[22] established the following expression for relaxation modulus:

$$G(t) = G_N^0 F(t) R(t) \tag{10}$$

$F(t)$ is the relaxation function of pure reptation (eq 1), and $R(t)$ represents the tube-renewal contribution as

$$R(t) = \frac{1}{N}\sum_{j=1}^{N} \exp\left(-4t \sin^2\left(\frac{j\pi}{2N}\right)/\pi^2\tau_w\right)$$

Neglecting the relaxation time distribution in the above functions, $F(t)$ and $R(t)$, and keeping only the dominant terms corresponding to $n = j = 1$, relation 10 becomes

$$G(t) = G_N^0 \exp(-t(\tau_d^{-1} + \tau_t^{-1})) \tag{11}$$

with τ_t given by relation 7 for $N \gg 1$.

The resulting terminal relaxation time τ is

$$\tau = (\tau_d^{-1} + \tau_t^{-1})^{-1} \tag{12}$$

For an N-chain isolated in an N_S-matrix, the reptation time τ_d is unchanged if the entanglement density is constant and the tube-renewal time τ_t follows relation 8. But, what happens for τ_t if the tube is constituted by chains with different lengths?

We have proposed[8] a constraint release function for an N_i-chain of the matrix, rewritten here as

$$R_i(t) = \exp\left(-\frac{t}{3}\tau_{wi}\right) \tag{13}$$

corresponding to

$$\tau_{wi} = \int_0^{+\infty} R_i(t)^3 \, dt \tag{14}$$

Considering n different lengths of chains, we suggested an average constraint release function $R(t)$ as

$$R(t) = \sum_{i=1}^{n} \phi_i R_i(t) \tag{15}$$

leading to an average constraint release time:

$$\tau_w = \int_0^{+\infty} R(t)^3 \, dt \tag{16}$$

The tube-renewal time τ_{tj} of an N_j-chain imbedded in such a tube is given by

$$\tau_{tj} = N_j^a \tau_w \tag{17}$$

with $a = 1.9$ (experimental) or 2 (theoretical).

For a binary blend, the tube-renewal times of the two components have the form

$$\tau_{ti} = kM_i^{a+b}\left[\phi_i^3 + 9\phi_i^2\phi_j\frac{M_j^b}{M_i^b + 2M_j^b} + 9\phi_i\phi_j^2\frac{M_j^b}{2M_i^b + M_j^b} + \phi_j^3\left(\frac{M_j}{M_i}\right)^b\right] \tag{18}$$

with $b = 2.3$ (experimental) or 2.5 (theoretical).

Thus, the relaxation times τ_1 and τ_2 in relation 5 can be obtained by using relations 12 and 18. They vary with concentration, and expressions 12 and 18 allow us to define the shift factors λ_i introduced in the quadratic experimental laws.

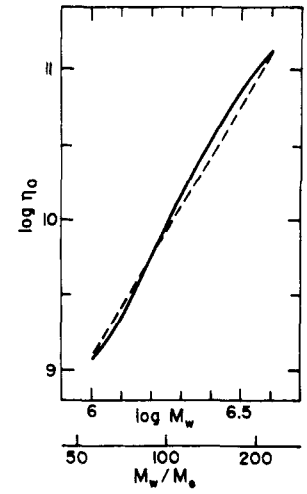

Figure 5. Theoretical variations of viscosity for a binary blend ($M_1 = 4 \times 10^6$; $M_2 = 10^6$) at 160 °C; (—) relation 21; (- - -) $\eta_0 \propto M_w^{3.4}$.

3. Zero-Shear Viscosity and Steady-State Compliance. From the relaxation modulus $G(t)$, we derive the zero-shear viscosity by

$$\eta_0 = \int_0^{+\infty} G(t) \, dt = G_N^0[\phi_1^2\tau_1 + (1 - \phi_1^2)\tau_2] \tag{19}$$

and the steady-state compliance by

$$J_e^0 = \eta_0^2 \int_0^t tG(t) \, dt = \frac{1}{G_N^0}\frac{\phi_1^2\tau_1^2 + (1 - \phi_1^2)\tau_2^2}{[\phi_1^2\tau_1 + (1 - \phi_1^2)\tau_2]^2} \tag{20}$$

Our data for polystyrene allows us to check the above expressions. We used experimental values of exponents and coefficients, i.e., $\tau_d = 2.3 \times 10^{-7}$ M$^{3.3}$ s,[8] $k = 1.4 \times 10^{-21}$ cgsu at $T = 160$ °C, $a = 1.9$ and $b = 2.3$ in relation 18, and $G_N^0 = 2 \times 10^6$ dyn cm^{-2}. On the other hand, owing to relaxation time distribution characterized by the average time $\tau_n = \eta_0/G_N^0$ and $\tau_v = \eta_0 J_e^{0\,32}$ and to the experimental determination of relaxation times,[8] the exact relations are

$$\eta_0 = \frac{1}{2}G_N^0[\phi_1^2\tau_1 + (1 - \phi_1^2)\tau_2] \tag{21}$$

$$J_e^0 = \frac{5}{2}\frac{1}{G_N^0}\frac{\phi_1^2\tau_1^2 + (1 - \phi_1^2)\tau_2^2}{[\phi_1^2\tau_1 + (1 - \phi_1^2)\tau_2]^2} \tag{22}$$

In effect, we have shown that for narrow fractions $\tau \simeq 2\tau_n$ and $J_e^0 G_N^0 \simeq 2.5$.

Figure 5 shows that for highly entangled binary blends relation 21 represents correctly experimental results ($\eta_0 \propto M_w^{3.4}$). But for weakly entangled blends, Figure 6 exhibits lower values of viscosity than the above power law. It can be noticed that some data[19] support a weak decrease of viscosity for the lowest concentration of 1-component if $M_2/M_e \leq 6$ but a discrepancy remains with relation 21. One of the main reasons for this might be the inadequacy of the power law $G_N'^0 \propto \phi^2$ for low values of ϕM.

Indeed, Graessley[32] studied the concentration dependence of reduced compliance J_{eR} for several solutions of linear polymers. He concluded that the steady-state compliance is proportional to the reciprocal of the first power of concentration at high enough concentrations for appreciable coil overlap to occur ($\phi M > M_e \simeq 2$–$3M_e$), but less than $\phi_c' = M_c'/M$ ($M_c' = 6$–$7M_e$). Our experimental results on plateau modulus, which varies as the reciprocal of J_e^0, are qualitatively consistent with a weaker than

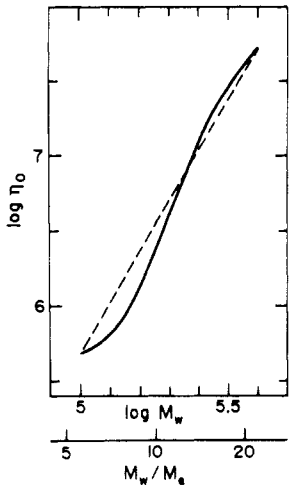

Figure 6. Theoretical variations of viscosity for a binary blend ($M_1 = 4 \times 10^5$; $M_2 = 10^5$) at 160 °C: (—) relation 21; (---) $\eta_0 \propto M_w^{3.4}$.

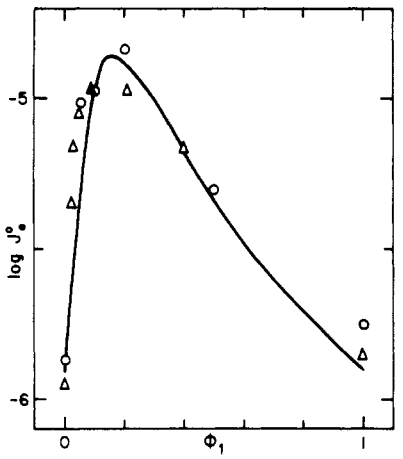

Figure 7. Variations of steady-state compliance for binary blends with same value of $M_1/M_2 = 4.2$: (—) relation 22; (Δ) ref 2, M_1 = 411 000 and M_2 = 97 200; (+) ref 36, M_1 = 670 000 and M_2 = 160 000.

quadratic power law for $M_c < \phi M \leq M_c'$. In Figures 2 and 4, the points lying in this range are above the curves. For the corresponding blends, the entanglement network of chains of the same length is not sufficiently dense. Thus, the tube-length fluctuations cannot be neglected.

Expression 22 is in good agreement with experimental data of J_e^0 (Figure 7). It describes fairly well the important effects of polydispersity and a weak variation with the molecular weight of the components. It is successful even in the case of very large ratios of molecular weights (see Figure 20, ref 8).

II. Polydisperse Samples

1. Relaxation Modulus $G(t)$. We consider a blend with p components of molecular weight decreasing from M_1 to M_p and terminal relaxation time decreasing from τ_1 to τ_p. Arguing in the same way as for binary blends, we postulate that for frequencies between τ_1^{-1} and τ_2^{-1} the temporary entanglement network is constituted by 1–1 chain contacts and the contribution to plateau modulus is therefore proportional to ϕ_1^2. Between τ_2^{-1} and τ_3^{-1}, an additional elastic response is provided by 1–2 and 2–2 type contacts, and the weight of their contribution is

$$(\phi_1 + \phi_2)^2 - \phi_1^2 = \phi_2^2 + 2\phi_1\phi_2 \tag{23}$$

With the same argument we derive the contribution to the interval $\tau_j^{-1} - \tau_{j+1}^{-1}$ as

$$(\sum_{k=1}^{j} \Phi_k)^2 - (\sum_{l=1}^{j-1} \Phi_l)^2 = \phi_j^2 + 2\phi_j \sum_{k=1}^{j-1} \phi_k \tag{24}$$

The lifetime of these entanglements is of the order of the shortest relaxation times of the chains involved in such contacts, then equal to τ_j.

If all the pure components have the same plateau modulus G_N^0 (this occurs for $M > M_c'$), we obtain a generalization of relation 5 for the relaxation modulus in the form

$$G(t) = G_N^0 \sum_{n=1}^{P} \phi_n(\phi_n + 2\sum_{k=1}^{n-1} \phi_k) \exp(-t/\tau_n) \tag{25}$$

For a whole sample, the molecular weight distribution is represented by the weight distribution function $P(M)$ such that $d\phi = P(M)\ d \ln M$. Then, the relaxation modulus has the following expression:

$$G(t) = 2G_N^0 \int_{-\infty}^{+\infty} \left[\int_{\ln M}^{+\infty} P(M)\ d \ln M\right] P(M) \exp(-t/\tau)\ d \ln M \tag{26}$$

2. Relaxation Times. For an N-chain in a whole polymer, the relaxation time τ obeys relation 12, where the reptation time τ_d is insensitive to the environment, provided that the entanglement density remains constant. On the other hand, the tube renewal τ_t, expressed by (relation 17)

$$\tau_t = N^a \tau_w \tag{27}$$

depends on the nature of the chains constituting the tube by means of the average constraint release time τ_w defined by relation 16. In that relation, the average constraint release function $R(t)$ is given by

$$R(t) = \int_{-\infty}^{+\infty} P(M) R(t,M)\ d \ln M \tag{28}$$

where $R(t,M) = \exp(-t/3\tau_w(M))$ and $\tau_w(M) = kM_e^a M^b$. Then

$$\tau_w = \int_{-\infty}^{+\infty} \left[\int_{-\infty}^{+\infty} P(M) \exp(-t/3kM_e^a M^b)\ d \ln M\right]^3 dt \tag{29}$$

We have checked the above relation, giving to parameters k, a, and b the experimental values used in section I. The two molecular weight distribution functions $P(M)$ were a symmetrical distribution (log-normal function)

$$P(M) = \frac{1}{\sigma(2\pi)^{1/2}} \exp\{-[(\ln M - \ln M_0)^2/2\sigma^2]\} \tag{30}$$

and a dissymmetrical distribution (Schulz–Zimm type)

$$P(M) = \frac{1}{\Gamma(Z+1)}[(Z+1)M/M_w]^{Z+1} \exp[-(Z+1)M/M_w] \tag{31}$$

The results are summarized in Table III and represented in Figure 8 in a reduced form. The waiting time $\tau_w(M_w)$ is the time expected for a monodisperse sample of molecular weight M_w—equal to the weight-average molecular weight of the distribution:

$$\tau_w(M_w) = kM_e^a M_w^b \tag{32}$$

The main features are (1) the waiting time τ_w is sensitive to the shape of the distribution and we can expect a strong effect for samples exhibiting a tail of very high or very low molecular weights and (2) there is no general relationship with a usual average molecular weight; however, $\tau_w(M_n) < \tau_w < \tau_w(M_w)$.

Table III
Effect of Polydispersity on the Average Waiting Time τ_w

$P = M_w/M_n$	$\tau_w/\tau_w(M_w)$ log normal	$\tau_w/\tau_w(M_n)$ log normal	$\tau_w/\tau_w(M_w)$ Schulz–Zimm
1	1	1	1
1.05	0.92	1.03	0.91
1.1	0.84	1.05	0.87
1.3	0.67	1.22	0.71
1.5	0.55	1.40	0.63
2	0.38	1.87	0.54
3	0.26	3.25	
4	0.21	5.09	
6	0.15	9.24	
10	0.10	19.95	

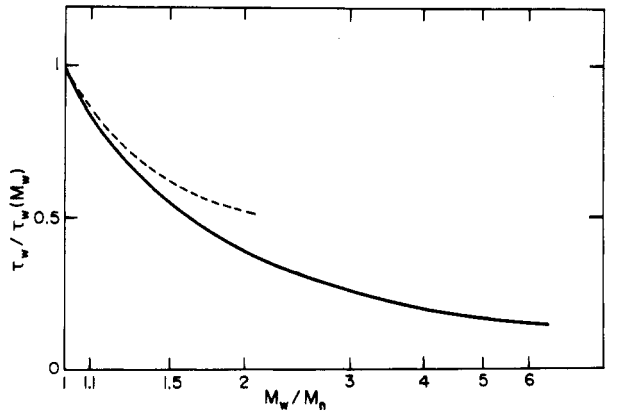

Figure 8. Average waiting time τ_w for continuous MWD as a function of the polydispersity P for two analytical distributions: (—) log normal; (- - -) Schulz–Zimm.

3. Zero-Shear Viscosity and Steady-State Compliance. The expressions of η_0 and J_e^0 derived from relation 26 are

$$\eta_0 = 2G_N^0 \int_{-\infty}^{+\infty} \left[\int_{\ln M}^{+\infty} P(M)\, d\ln M \right] \tau(M) P(M)\, d\ln M \tag{33}$$

$$J_e^0 = \frac{2G_N^0}{\eta_0^2} \int_{-\infty}^{+\infty} \left[\int_{\ln M}^{+\infty} P(M)\, d\ln M \right] \tau^2(M) P(M)\, d\ln M \tag{34}$$

The calculated values of viscosity η_0 by relation 33 are shown in Figures 9 and 10 for two analytical molecular weight distributions (relations 30 and 31), varying the average molecular weights and the broadness of the distribution. We observe essentially (1) a relationship η_0 vs. M_w very close to that described for narrow distribution samples, provided that the shape and the broadness of the distribution are the same for all the samples. The slope increases slightly from 3.4 to 3.8 with polydispersity. The values of viscosity change with the shape of the distribution, as can be seen in Tables IV and V by comparing at the same value of polydispersity index $P = M_w/M_n$ (P = 2 for instance). (2) For the lowest values of P, the decrease of viscosity at the same M_w is clear. This is a consequence of the effect of the low molecular weight tail on the average waiting time τ_w.

The increase of the average lifetime of every constraint due to the presence of large chains is offset by the decrease induced by the short chains. This effect is clearly emphasized at low polydispersities and low M_w but remains for the high molecular weights. Experimental results on broad distribution polystyrenes[6] support clearly the decrease of viscosity with polydispersity (Figure 11). In this narrow range of M_w values, a power law $\eta_0 \propto M_w^{4.95}$ holds.

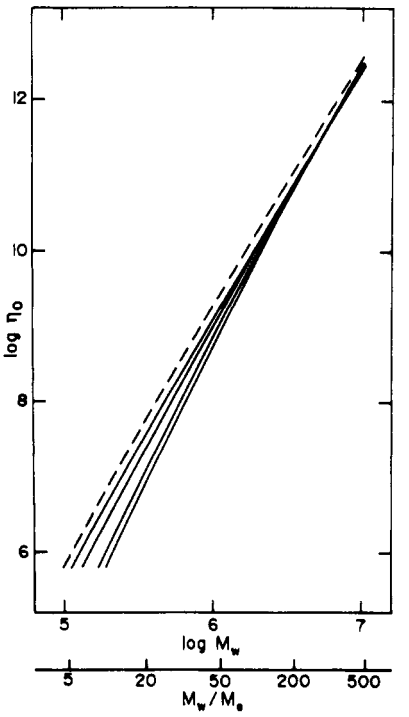

Figure 9. Theoretical variations of viscosity for log-normal distribution polystyrenes at T = 160 °C (relation 33′) for different values of P: (- - -) monodisperse; (—) from left to right, P = 1.1, 2, 6, 10.

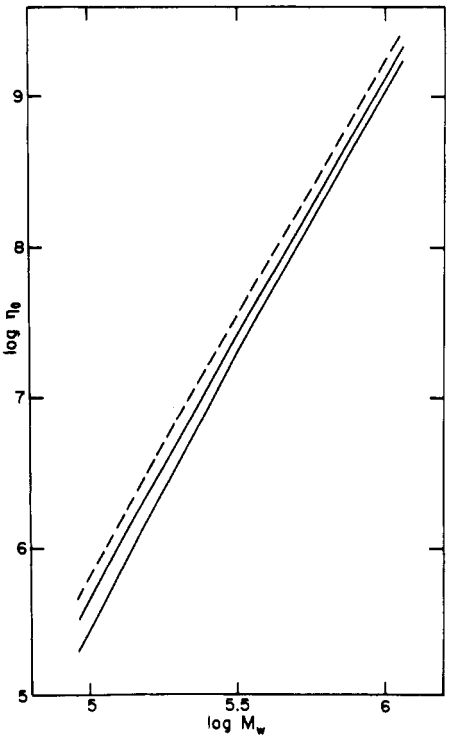

Figure 10. Theoretical variations of viscosity for Schulz–Zimm distribution polystyrenes at T = 160 °C (relation 33′) for different values of P: (- - -) monodisperse; (—) P = 1.05, 2.

This high exponent was obtained for P varying from 2 to 5.

According to the range of P and M_w values, the exponent can vary in a large scale. Figure 9 shows, however, that for $M_w > 100M_e$ and whatever the polydispersity, the curves merge, leading to an exponent close to 3.4. This is supported by data on HDPE samples[4] for which P varies from 6.54 to 15.4 and, at the same time, M_w/M_e varies from 55 to 128.

Table IV
Zero-Shear Viscosity and Steady-State Compliance for Log-Normal Distribution Polystyrenes[a]

	$P = 1$		$P = 1.1$		$P = 2$		$P = 6$		$P = 10$	
log M_w	log η_0	log J_e^0	log η_0	log J_e^0	log η_0	log J_e^0	log η_0	log J_e^0	log η_0	log J_e^0
5	5.81	−5.98	5.62	−5.79	5.30	−5.06	4.88	−4.21	4.69	−3.83
5.2	6.52		6.34	−5.77	6.07	−4.99	5.69	−4.16	5.51	−3.79
5.4	7.22		7.05	−5.75	6.82	−4.92	6.50	−4.09	6.32	−3.74
5.6	7.91		7.74	−5.74	7.56	−4.83	7.29	−4.02	7.13	−3.68
5.8	8.59		8.42	−5.73	8.29	−4.75	8.07	−3.93	7.93	−3.61
6	9.26		9.10	−5.72	9.00	−4.66	8.85	−3.83	8.72	−3.53
6.2	9.93		9.77	−5.715	9.70	−4.57	9.61	−3.72	9.50	−3.43
6.4	10.6		10.44	−5.71	10.40	−4.49	10.36	−3.60	10.28	−3.33
6.6	11.26		11.10	−5.71	11.08	−4.42	11.10	−3.46	11.05	−3.21
6.8	11.92		11.76	−5.705	11.76	−4.36	11.84	−3.32	11.80	−3.08
7	12.59		12.43	−5.705	12.43	−4.31	12.56	−3.18	12.55	−2.935

[a] Calculated from relations 33′ and 34′ (T = 160 °C).

Table V
Zero-Shear Viscosity and Steady-State Compliance for Schulz-Zimm Distribution Polystyrenes[a]

	$P = 1$		$P = 1.05$		$P = 1.09$		$P = 1.5$		$P = 2$	
log M_w	log η_0	log J_e^0	log η_0	log J_e^0	log η_0	log J_e^0	log η_0	log J_e^0	log η_0	log J_e^0
5	5.81	−5.98	5.68	−5.885	5.64	−5.81	5.515	−5.48	5.47	−5.33
5.2	6.52		6.40	−5.875	6.36	−5.795	6.25	−5.44	6.22	−5.29
5.4	7.22		7.10	−5.87	7.06	−5.78	6.98	−5.41	6.95	−5.24
5.6	7.91		7.79	−5.86	7.76	−5.77	7.69	−5.37	7.67	−5.20
5.8	8.59		8.47	−5.86	8.44	−5.765	8.38	−5.335	8.38	−5.16
6	9.26		9.14	−5.855	9.11	−5.76	9.07	−5.31	9.07	−5.12
6.2	9.93		9.81	−5.85	9.78	−5.75	9.75	−5.29	9.76	−5.09
6.4	10.6		10.48	−5.85	10.45	−5.75	10.42	−5.275	10.44	−5.07
6.6	11.26		11.14	−5.85	11.12	−5.75	11.09	−5.265	11.11	−5.05
6.8	11.92		11.80	−5.85	11.78	−5.75	11.76	−5.26	11.78	−5.04
7	12.59		12.47	−5.85	12.44	−5.75	12.42	−5.25	12.44	−5.03

[a] Calculated from relations 33′ and 34′ (T = 160 °C).

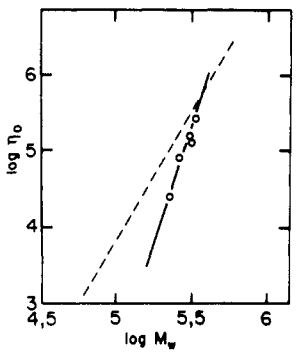

Figure 11. Experimental results for broad distribution polystyrenes at T = 200 °C (ref 6). The dotted line represents the viscosity of fractions.

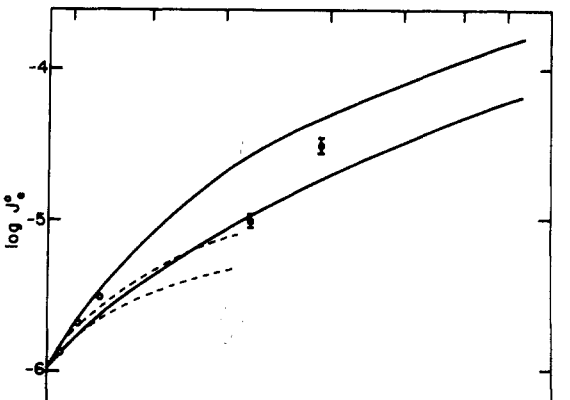

Figure 12. Theoretical variations of steady-state compliance (relation 34′) as a function of P for two analytical distributions: (—) log normal and (- - -) Schulz–Zimm. In each case, the upper curve is for $M = 10^6$ and the lower curve for $M = 10^5$.

The steady-state compliance is very sensitive to the MWD, mainly to the high molecular weight tail. It appears in Figure 12 that relation 34 describes fairly well the variations of J_e^0: a strong increase with polydispersity and a noticeable difference according to the shape of distribution. Our model adds a slight effect of the molecular weight.

The empirical relations take into account only the average molecular weights[33] and therefore are not precise enough to describe all the above effects. For log-normal distributions, they give power laws for the variations of J_e^0 vs. polydispersity P, leading to straight lines in Figure 12. Such linear representations are consistent with the theoretical curves of Figure 12 in a limited range of polydispersity, with slopes varying from 3 to 5, for $M_w/M_n < 3$. For example, the slope of value 4 represents the following relation:

$$J_e^0 \propto \frac{M_z M_{z+1}}{M_n M_w}$$

Table VI
Viscosities of Commercial Polystyrenes[5]

sample	M_w	P	log η_0 exptl	log η_0 calcd (rel 33′)
A	225 000	3.57	6.27	6.46
B	260 000	3.77	6.62	6.63
C	312 000	5.03	6.97	6.90
D	302 000	2.40	7.02	7.15
E	333 000	2.16	7.37	7.25

No representation is valid for all shapes of MWD and all values of polydispersity.

The polydispersity effects we have calculated from relations 33 and 34 allow us to derive the theoretical behavior of strictly monodisperse samples (P = 1). Using experimental data for narrow fractions ($P < 1.1$),[8] we have cal-

Table VII
Viscosity and Compliance of Narrow and Broad Distribution Polystyrenes[a]

sample	M_w	P	log η_0 exptl	log η_0 calcd (rel 33′)	log J_e^0 exptl	log J_e^0 calcd (rel 34′)
F11	110 000	1.05	5.90	5.82	−5.90	−5.89
F20	200 000	1.06	6.78	6.73	−5.86	−5.87
F39	390 000	1.10	7.64	7.75	−5.80	−5.77
F90	900 000	1.12	8.40	9.05	−5.68	−5.72
F270	2 700 000	1.20	10.20	10.64	−5.50	−5.6
PS126C	227 000	2.17	6.7	6.56	−5.0	−4.9
PS8	390 000	2.9	7.4	7.45	−4.5	−4.6

[a] T = 160 °C.

culated the prefactors in relations 33 and 34 by fitting theoretical curves for P = 1.05 to those data. We derive the following values of terminal parameters, at T = 160 °C, for monodisperse polystyrenes: $\tau_d = 3.2 \times 10^{-17} M^{3.3}$s; $\tau_t = 2 \times 10^{-21} M^{4.2}$s; $\eta_0 = 6.6 \times 10^{-12} M^{3.4}P$; $J_e^0 = 1.05 \times 10^{-6}$ cm^2 dyn^{-1}; $G_N^0 = 2 \times 10^6$ dyn cm^{-2}.

The product $G_N^0 J_e^0$, which is a measure of the breadth of the terminal relaxation spectrum, is equal to 2.1. This value is very close to those obtained for very narrow distribution polybutadienes and polyisoprenes[25] calculated by Graessley,[22] who considers a distribution of reptation and tube-renewal times for a monodisperse polymer. Moreover, the relaxation times $\tau_d(M)$, $\tau_t(M)$, and therefore $\tau(M)$ in relations 33 and 34 are average relaxation times, twice the average time $\tau_n = \eta_0/G_N^0$ for narrow fractions. In the same way as for binary blends, the precise relations we have used to check our model are slightly different from theoretical relations:

$$\eta_0 = G_N^0 \int_{-\infty}^{+\infty} \left[\int_{-\infty}^{+\infty} P(M)\, \mathrm{d} \ln M \right] \tau(M) P(M)\, \mathrm{d} \ln M \tag{33′}$$

$$J_e^0 = 2.1 \frac{G_N^0}{\eta_0^2} \int_{-\infty}^{+\infty} \left[\int_{-\infty}^{+\infty} P(M)\, \mathrm{d} \ln M \right] \tau^2(M) P(M)\, \mathrm{d} \ln M \tag{34′}$$

Date reported in Table VI show that the values of viscosity calculated from relation 33′ are in agreement with experimental results, provided that the isothermal viscosity of narrow fractions, determined by different techniques, are adjusted. Here, the experimental values are corrected, fitting the viscosity of narrow fractions reported in ref 6 with our results[18] at 160 °C.

We report in Table VII results we have obtained on the fractions of polystyrene[8] and two broad distribution commercial polystyrenes. We have considered a Schulz–Zimm distribution for fractions and a log-normal distribution for commercial samples. The predictions of relations 33′ and 34′ are quite acceptable. We notice an important gap for the viscosities of fractions F90 and F270. Does this discrepancy come from the fact that for high molecular weights (where pure reptation is expected) relaxation times scale in agreement with reptation theory ($\tau = \tau_d \propto M^3$)? In that case the experimental law $\tau \propto M^{3.4}$ would result from the combination of reptation, tube-renewal, and tube-length fluctuation[34,35] for chains weakly entangled.

Conclusion

We have presented a simple model of relaxation including chain reptational motion and tube-renewal process in order to describe the effects of molecular weight distribution on the terminal rheological properties. We have shown that polydispersity leads to a decrease of viscosity. The experimental power law $\eta_0 \propto M_w^{3.4}$ is therefore roughly valid for very close polydispersities, except for high molecular weights, namely $M_w > 100M_e$. Moreover, the shape of the MWD has a weak effect on viscosity. On the contrary, our model predicts a strong effect of the shape on steady-state compliance: J_e^0 for a binary blend of fractions may be very different from that of a broad distribution sample with the same value of P. The variations of J_e^0 have been calculated in a wide range of polydispersities with good agreement with experimental results. Zero-shear viscosity and steady-state compliance of linear polymers can be calculated for any MWD from relations 12, 27, 29, 33, and 34 if the behavior of monodisperse samples is known. However, if the distribution contains very low molecular weights ($M \leq 2M_e$), the effect of chain ends on the monomeric mobility and the decrease of entanglement density should be taken into account.

From these polydispersity effects we have derived the behavior of strictly monodisperse samples and shown that one has to take into account a distribution of terminal relaxation times, which is measured by the product $G_N^0 J_e^0$ = 2.1. Considering such a distribution and including other modes of relaxations, that is, tube-length fluctuations and motions between entanglement points, one would be able to explain the rheological behavior over the whole relaxation spectrum from the terminal to the transition regions.

Registry No. Polystyrene, 9003-53-6.

References and Notes

(1) Montfort, J. P.; Marin, G.; Arman, J.; Monge, Ph. *Polymer* **1978**, *19*, 277.
(2) Prest, M. W.; Porter, R. S. *Polym. J. (Tokyo)* **1973**, *4*, 154.
(3) Masuda, T.; Kitagawa, K.; Inoue, T.; Onogi, S. *Macromolecules* **1970**, *3*, 116.
(4) Miltz, J.; Ram, A. *Polym. Eng. Sci.* **1973**, *13*, 273.
(5) Marin, G. Thèse 3e cycle, Université de Pau, 1975.
(6) Rudin, A.; Chee, K. K. *Macromolecules* **1973**, *6*, 613.
(7) Mills, J. N.; Nevin, A. *J. Polym. Sci., Polym. Phys. Ed.* **1971**, *9*, 267.
(8) Montfort, J. P.; Marin, G.; Monge, Ph. *Macromolecules* **1984**, *17*, 1551.
(9) Bogue, D. C.; Masuda, T.; Einaga, Y.; Onogi, S. *Polym. J. (Tokyo)* **1970**, *1*, 563.
(10) Graessley, W. W. *J. Chem. Phys.* **1971**, *54*, 5143.
(11) Prest, W. M. *Polym. J. (Tokyo)* **1973**, *4*, 163.
(12) Masuda, T.; Takahashi, M.; Onogi, S. *Appl. Polym. Symp.* **1973**, *20*, 49.
(13) Hong, S. D.; Soong, D.; Shen, M. *J. Appl. Phys.* **1977**, *48*, 4019.
(14) Hong, S. D.; Hansen, D. R.; Williams, M. C.; Shen, M. *J. Polym. Sci., Polym. Phys. Ed.* **1977**, *15*, 1869.
(15) Soong, D.; Shen, M.; Hong, S. D. *J. Rheol.* **1979**, *23*, 301.
(16) Soong, D.; Shyu, S. S.; Shen, M. *J. Macromol. Sci., Phys.* **1981**, *19*, 49.
(17) Kurata, M. *Macromolecules* **1984**, *17*, 895.
(18) Doi, M.; Edwards, S. F. *J. Chem. Soc., Faraday Trans. 2* **1978**, *74*, 1789, 1802, 1818.
(19) Watanabe, H.; Kotaka, T. *Macromolecules* **1984**, *17*, 2316.
(20) Watanabe, H.; Sakamoto, T.; Kotaka, T. *Macromolecules* **1985**, *18*, 1008.
(21) Marrucci, G. *J. Polym. Sci., Polym. Phys. Ed.* **1985**, *23*, 159.
(22) Graessley, W. W. *Adv. Polym. Sci.* **1982**, *47*, 67.
(23) Montfort, J. P. Thèse d'Etat, Université de Pau, 1984.
(24) Ferry, J. D. *Viscoelastic Properties of Polymers*, 3rd ed.; Wiley: New York, 1980.
(25) Raju, V. R.; Menezes, E. V.; Marin, G.; Graessley, W. W. *Macromolecules* **1981**, *14*, 1668.

(26) Masuda, T.; Toda, N.; Aoto, Y.; Onogi, S. *Polym. J. (Tokyo)* **1972**, *3*, 315.
(27) Nemoto, N.; Ogawa, T.; Odani, H.; Kurata, M. *Macromolecules* **1972**, *5*, 641.
(28) Montfort, J. P.; Marin, G.; Monge, Ph. *Macromolecules* **1986**, *19*, 393.
(29) Klein, J. *Macromolecules* **1978**, *11*, 852.
(30) Klein, J. *Polym. Prepr. (Am. Chem. Soc., Div. Polym. Chem.)* **1981**, *22*, 105.
(31) Klein, J. *Macromolecules* **1986**, *19*, 105.
(32) Graessley, W. W. *Adv. Polym. Sci.* **1974**, *16*, 1.
(33) Agarwal, P. K. *Macromolecules* **1979**, *12*, 342.
(34) Doi, M. *J. Polym. Sci., Polym. Phys. Ed.* **1980**, *18*, 1005.
(35) Lin, Y. H. *Macromolecules* **1984**, *17*, 2846.
(36) Marin, G. Thèse d'Etat, Université de Pau, 1977.
(37) Masuda, T.; Yoshimatsu, S.; Takahashi, M.; Onogi, S. *Polym. Prepr. Jpn.* **1983**, *32*, 2365.
(38) Watanabe, H.; Sakamoto, T.; Kotaka, T. *Macromolecules* **1985**, *18*, 1436.
(39) Marin, G.; Montfort, J. P.; Monge, Ph. *J. Non-Newtonian Fluid Mech.*, in press.

Viscoelastic Properties and Molecular Structure of Amorphous Selenium

Gabriel Faivre* and Jean-Louis Gardissat

Laboratoire PMTM, CNRS, 93430 Villetaneuse, France. *Received December 17, 1985*

ABSTRACT: The transient and dynamical linear viscoelastic properties of pure amorphous selenium are measured in the temperature range 35–70 °C, and new ideas are proposed to explain them within the framework of the equilibrium polymerization theory. Our experimental results confirm and improve earlier results of Eisenberg and co-workers in establishing more firmly that the viscoelastic response of selenium is similar to that of a narrow molecular weight distribution polymer of low degree of polymerization. The proposed theory shows that a dynamical polymer, as we believe amorphous selenium is, behaves approximately like an ordinary narrow molecular weight distribution polymer. This may solve the problem of reconciling equilibrium polymerization with viscoelastic properties of selenium.

Introduction

The molecular structure of liquid selenium is not completely understood. One generally agrees that it is of a polymeric nature. Recently again, this opinion has been corroborated by careful X-ray[1,2] and neutron[3] diffusion investigations of the structure in the liquid and amorphous states (here, and in what follows, "amorphous state" denotes the state of the liquid after it has been quenched to a temperature higher than, but close to, the glass transition temperature T_g = 30 °C). However, very little is known about the molecular weight distribution of this polymeric liquid.[4] The purpose of this paper is to present the results of an investigation of the linear viscoelastic properties of amorphous selenium and the newly drawn conclusions about the molecular structure of the liquid that can be deduced from the careful discussion of these results.

The viscoelastic properties of amorphous selenium have already been studied in the past by Eisenberg, Tobolsky, and Teter.[5,6] Nevertheless, several reasons incited us to reexamine the subject.

First, progress has obviously been made in the knowledge of viscoelastic properties of polymers since the work of Eisenberg and co-workers. The present situation in this field is very well summed up by the book of Ferry,[7] to which we shall frequently refer. Our main motivation, however, was that the real state of knowledge of liquid selenium has become clearer over the past few years.

In 1959, following precursory papers of Gee[8] and co-workers, Tobolsky and Eisenberg[9] produced a theory of the polymerization of liquid sulfur, called "equilibrium polymerization". This theory succeeded in describing the well-known transition of liquid sulfur near 160 °C, the temperature at which sulfur reversibly transforms from a nonpolymeric liquid, almost exclusively composed of S_8 ring molecules, to a heavily polymerized liquid. The success of this theory has recently been confirmed again by the work of Wheeler, Kennedy, and Pfeuty.[10]

In 1960, another article by Eisenberg and Tobolsky[11] put forward the idea that selenium may obey the same laws of polymerization as sulfur, in spite of the fact that no polymerization transition analogous to that of sulfur is observed in liquid selenium. At that time, these authors had at their disposal experimental results published by Briegleb[12] in 1929 on the selective solubility of selenium in carbon disulfide, according to which Se_8 ring molecules are present in the liquid in proportions that depend on temperature but that are generally greater than 10%. From these results, Eisenberg and Tobolsky predicted that the polymerization transition of selenium should occur near 80 °C. This fact, of course, is not observed, but the authors concluded that the chemical reactions that are responsible for the equilibrium polymerization are critically slowed down when above this temperature.

For a relatively long time, the views of Eisenberg and Tobolsky were considered by many authors as firmly established. But nowadays, one has good reason to think that the experiments of Briegleb were spoiled by serious artifacts.[13] Furthermore, no other experimental method succeeded in proving unambiguously the existence of Se_8 ring molecules in liquid or amorphous selenium. Thus, these molecules, if present in liquid selenium, are in very small concentration. Consequently, the polymerization transition, if it exists, is relegated to a very low temperature and is, in any case, only potential. The essential process of the equilibrium polymerization no longer involves the small ring molecules: it lies in the fact that the chain molecules directly undergo chemical reactions of dissociation or concatenation. The situation is then similar to that described theoretically by Jacobson and Stockmayer[14] for some organic polymers.

In conclusion, the fact that the numerous efforts to prove the existence of Se_8 molecules in liquid selenium have been unsuccessful leads us to reject the quantitative conclusions of the Eisenberg and Tobolsky article published in 1960

0024-9297/86/2219-1988$01.50/0